Tetrahedron 66 (2010) 8714–8721

Contents lists available at ScienceDirect

Tetrahedron

journal homepage: www.elsevier.com/locate/tet

Evaluation of the binding ability of a macrobicyclic receptor for anions by potentiometry and molecular dynamics simulations in solution

Sílvia Carvalho [a,b], Rita Delgado [a,c,*], Vítor Félix [b,*]

[a] Instituto de Tecnologia Química e Biológica, UNL, Av. da República—EAN, 2780-157 Oeiras, Portugal
[b] Departamento de Química, CICECO, and Secção Autónoma de Ciências da Saúde, Universidade de Aveiro, 3810-193 Aveiro, Portugal
[c] Instituto Superior Técnico, Departamento de Química, Av. Rovisco Pais, 1049-001 Lisboa, Portugal

ARTICLE INFO

Article history:
Received 23 June 2010
Received in revised form 31 August 2010
Accepted 3 September 2010
Available online 15 September 2010

Keywords:
Supramolecular chemistry
Cryptand
Binding constants
Molecular dynamics simulation
Anionic recognition

ABSTRACT

The macrobicycle derived from bis-tren and containing diphenoxy groups as spacers, L^1, was synthesized and used as receptor for anions. The binding ability of the new receptor for some aromatic carboxylates [phthalate (ph^{2-}), isophthalate (iph^{2-}), terephthalate (tph^{2-}), benezenetricarboxylate (btc^{3-}), and the herbicide 4-amino-3,5,6-trichloro-2-pyridinecarboxylate ($ATCP^-$)], and the aliphatic cyclohexanetricarboxylate (ch^{3-}) anions was evaluated by potentiometric measurements and molecular dynamic simulation in solution. The association constants were determined by potentiometry in H_2O/MeOH (1:1 v/v) at 298.2 K and 0.10 mol dm^{-3} in KCl. The strongest association was found with btc^{3-} anion and the effective binding constants at pH 5.5 follow the order: $btc^{3-} > tph^{2-} > ph^{2-} \approx iph^{2-} > ch^{3-} \approx ATCP^-$. Molecular dynamics simulations carried out for the associations of $(H_6L^1)^{6+}$ with btc^{3-}, tph^{2-} and iph^{2-} in the same mixture of solvents indicated that these anions interact with the receptor by a combination of electrostatic and multiple N–H···O=C hydrogen bond interactions. It was also verified that in the recognition process the tph^{2-} remained encapsulated over the entire time of simulation while the btc^{3-} is partially inserted into the receptor cavity with one carboxylate group largely exposed to water solvent molecules, and iph^{2-} anion exhibited an intermediate binding behaviour. The free energy difference between btc^{3-} and iph^{2-} associations estimated by free energy calculations is in excellent agreement with the difference found from the experimental values for the corresponding association constants, which indicates that the unconstrained molecular dynamics simulations carried out with these two anions are realistic pictures of their molecular recognition processes.
© 2010 Elsevier Ltd. All rights reserved.

1. Introduction

New techniques and tools to detect and remove pollutants contributing to the environmental degradation are absolutely required, not only for metal ions but also for anions. For instance, certain anions and pesticides or herbicides are known to cause water eutrophication and ground degradation.[1] In spite of the negative features, anions are fundamental compounds in pharmaceutical, food and plastic industries, and for the function and regulation of many biological processes, consequently they are essential to life. Supramolecular chemistry strongly contributed, and continues to contribute, to such new tools with the design of receptors, the investigation of their recognition ability and the selection of those capable to sense and uptake anionic substrates.[1–4]

Among the synthetic receptors, macrobicycles or cryptands is one of the most suitable class of compounds for recognition studies due to their rigidity and pre-organization.[4–6] Polyammonium cryptands have been successfully used in the recognition of inorganic anions, such as halogenates, nitrate, sulfate, phosphate, perchlorate, and short chain carboxylate anions like acetate, oxalate and malonate.[7–15] The recognition of aromatic carboxylate anions by this type of receptors is still scarce and the work of Lehn et al.[7] is one of the rare reports in which an aromatic dicarboxylate anion, the terephthalate, is shown inserted into the polyammonium cryptand cavity. In fact, macrocycles are the mostly used receptors for binding of carboxylate anions.[2,16–18]

In our previous studies, polyaza macrocycles incorporating one aromatic ring as the spacer and different number of $-NH_2^+$ moieties as potential binding sites were used as receptors of aromatic anions. They were found too small or/and too flexible to lead to high binding affinities or selectivity.[19,20] Taking into account our previous achievement, we designed a new receptor (L^1) with the same functional groups (amines) and type of aromatic spacers, but with a three-dimensional and larger cavity by incorporation of diphenoxy groups as spacers and a third bridge covalently bound into the backbone of the macrocycle (Scheme 1). The various protonated forms of the receptor $(H_nL^1)^{n+}$ were used for the binding of mono-,

* Corresponding authors. Tel.: +351 21 446 9737; fax: +351 21 441 1277; e-mail addresses: delgado@itqb.unl.pt (R. Delgado), vitor.felix@ua.pt (V. Félix).

0040-4020/$ – see front matter © 2010 Elsevier Ltd. All rights reserved.
doi:10.1016/j.tet.2010.09.006

di- and tricarboxylate anions ($ATCP^{-}$, ph^{2-}, iph^{2-}, tph^{2-}, btc^{3-} and ch^{3-}, see Scheme 1) in H_2O/MeOH (1:1 v/v) solution. The binding ability evaluation was carried out by potentiometric technique. Further insights into the molecular recognition process between the receptor and three aromatic carboxylate anions (iph^{2-}, tph^{2-} and btc^{3-}) were undertaken by molecular dynamics simulations (MD) in periodic boxes of H_2O/MeOH (1:1 v/v) solvent molecules.

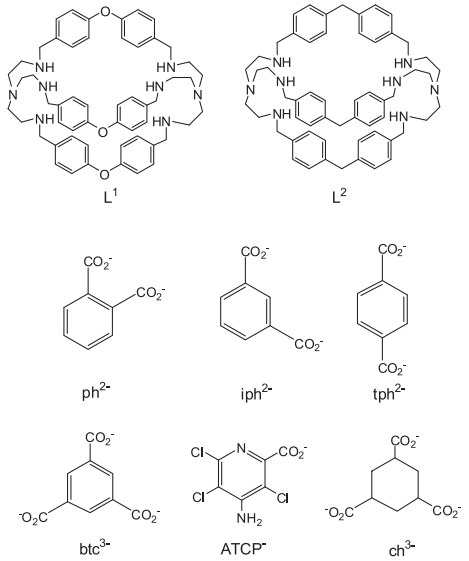

Scheme 1. Cryptands and anions discussed in this work.

2. Results and discussion

2.1. Synthesis of the receptor

The cryptand (L^1) was synthesized by the condensation of tris(2-aminoethyl)amine (tren) with 4-(4-formylphenoxy)benzaldehyde at rt, as reported for similar cases.[21] The pure compound in its hexaprotonated form was obtained in only 30% yield. The 4-(4-formylphenoxy) benzaldehyde was prepared using described procedures.[22]

2.2. Protonation constants of L^1

The acid–base reactions of L^1 were studied by potentiometry in H_2O/MeOH (1:1 v/v) solution, at 298.2 K and 0.10 mol dm^{-3} in KCl, and the protonation constants determined are collected in Table 1. The values for all basic centres could be determined by the technique used, except the last one due to its very low value. The first six constants have high values and they have similar magnitude in pairs, as they correspond to protonation of amine centres at alternating positions in the macrobicyclic backbone, far from each other, and therefore the difference in values for each pair are mainly due to statistical factors. On the other hand, the last two constants (only one determined), which correspond to protonation of tertiary amines, undergo the effect of the nearby three ammonium charges, and consequently present very low values.

Table 1
Overall ($\log \beta_i^H$) and stepwise ($\log K_i^H$) protonation constants of L^1 in H_2O/MeOH (1:1 v/v) solution. T=298.2 K; I=0.10 mol dm^{-3} in KCl

Equilibrium reaction	$\log \beta_i^{Ha}$	$\log K_i^H$
$L^1+H^+ \rightleftharpoons (HL^1)^+$	9.40(1)	9.40
$(HL^1)^+ + H^+ \rightleftharpoons (H_2L^1)^{2+}$	18.14(1)	8.74
$(H_2L^1)^{2+} + H^+ \rightleftharpoons (H_3L^1)^{3+}$	26.07(1)	7.93
$(H_3L^1)^{3+} + H^+ \rightleftharpoons (H_4L^1)^{4+}$	33.30(1)	7.23
$(H_4L^1)^{3+} + H^+ \rightleftharpoons (H_5L^1)^{5+}$	39.63(1)	6.33
$(H_5L^1)^{5+} + H^+ \rightleftharpoons (H_6L^1)^{6+}$	45.46(1)	5.83
$(H_6L^1)^{6+} + H^+ \rightleftharpoons (H_7L^1)^{7+}$	47.40(2)	1.94

[a] Values in parentheses are standard deviations on the last significant figure.

The hexaprotonated form of the cryptand, $(H_6L^1)^{6+}$, is the main species in solution at the 2.5–5.5 pH range, as shown in the distribution diagram presented in Fig. 1. This species, due to its high charge, strongly contributes to maximize the electrostatic interactions with the anionic substrate.

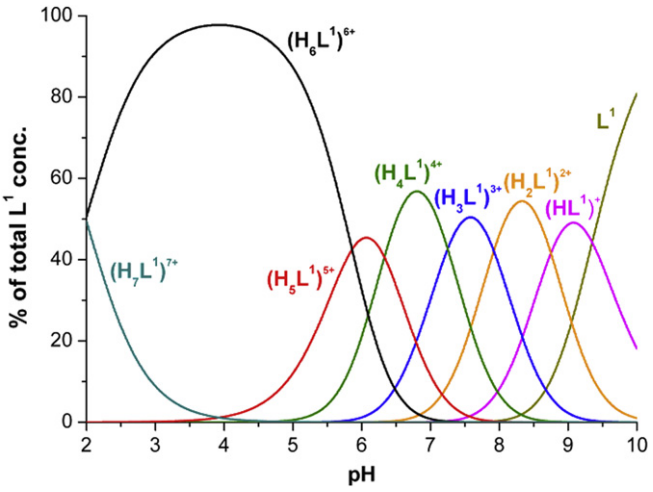

Fig. 1. Species distribution diagram of the receptor in H_2O/MeOH (1:1 v/v) solution. $C_{L^1} = 3.0 \times 10^{-3}$ mol dm^{-3}.

2.3. Binding studies in solution (potentiometric measurements)

Potentiometry is the most accurate technique for the quantitative evaluation of equilibrium constants of complicated systems in solution. Since receptors as well as anions have different degrees of protonation, the formation of associated species with different number of protons is expected and verified in our case. Indeed, the association constants of $(H_nL^1)^{n+}$ with the various carboxylate anions were determined in the experimental conditions already described for the protonation studies and the HYPERQUAD program was also used,[23] see Table 2. The protonation constants of the anionic substrates at the same experimental conditions were also determined and are shown in Table S1 of Supplementary data.

Only 1:1 receptor to substrate species of the type $[H_nL^1A]^{n-i}$ were found with all the anions studied, although with different protonation states (n from 1 to 8), as shown in Fig. 2 for the receptor/btc^{3-} system. The $[H_6L^1(btc)]^{3+}$ is the main species in the large pH range of 4.5–7.5, reaching ≈85% at pH=5.5. However as this associated entity covers a large pH range it can be formed by the reaction of several receptor and anion species of different protonation states such as between $(H_5L^1)^{5+}+HA^{2-}$ or/and $(H_6L^1)^{6+}+A^{3-}$. This fact renders the calculation of the stepwise constants a complicated process. In order to be sure of the equilibria involved at a certain pH the effective association constants, $K_{eff}=\Sigma[H_{i+n}AL]/(\Sigma[H_iA]\cdot\Sigma[H_nL])$, were determined,[4,24,25] and in Fig. 3 the plot of these constants for the studied systems are shown.

The effective constants of the receptor $(H_nL^1)^{n+}$ with the anionic substrates at pH 5.5 follow the order $btc^{3-}>tph^{2-}>ph^{2-}\approx iph^{2-}>ch^{3-}\approx ATCP^{-}$, see Fig. 3, being the values very high for the first two anions. Two different behaviours are observed for the associated entities formed with these anions in function of the pH. For the associations with btc^{3-}, tph^{2-}, iph^{2-} and ch^{3-}, the curves of log K_{eff} versus pH have a well-defined maximum indicating that electrostatic interactions play an important role in the binding. For the ph^{2-} and $ATCP^{-}$ associations, the effective constants have the same value in a large pH range,

Table 2
Overall association constants ($\log \beta_{H_hL_lA_a}$)[a] for the equilibria of $(H_nL^1)^{n+}$ with the indicated anions in H_2O/MeOH (1:1 v/v) solutions. I=0.10 mol dm^{-3} in KCl at T=298.2 K

Equilibrium process	ATCP$^-$	ph^{2-}	iph^{2-}	tph^{2-}	btc^{3-}	ch^{3-}
$8H^+ + L^1 + A^{i-} \rightleftarrows [H_8L^1A]^{(8-i)}$	—	—	—	—	58.37(6)	–
$7H^+ + L^1 + A^{i-} \rightleftarrows [H_7L^1A]^{(7-i)}$	—	54.27(4)	52.75(6)	54.23(5)	55.44(1)	54.27(3)
$6H^+ + L^1 + A^{i-} \rightleftarrows [H_6L^1A]^{(6-i)}$	48.55(2)	49.51(2)	49.29(1)	50.32(2)	51.16(1)	49.42(1)
$5H^+ + L^1 + A^{i-} \rightleftarrows [H_5L^1A]^{(5-i)}$	42.59(3)	43.22(3)	42.54(3)	42.9(1)	43.72(6)	42.07(9)
$4H^+ + L^1 + A^{i-} \rightleftarrows [H_4L^1A]^{(4-i)}$	36.23(2)	36.28(4)	35.39(5)	36.03(8)	36.37(6)	35.46(6)
$3H^+ + L^1 + A^{i-} \rightleftarrows [H_3L^1A]^{(3-i)}$	28.91(3)	28.96(4)	—	—	28.4(1)	—
$2H^+ + L^1 + A^{i-} \rightleftarrows [H_2L^1A]^{(2-i)}$	20.84(3)	—	—	—	—	—
$H^+ + L^1 + A^{i-} \rightleftarrows [HL^1A]^{(1-i)}$	11.96(4)	—	—	—	—	—

[a] Values in parentheses are standard deviations on the last significant figure. A denotes the anion.

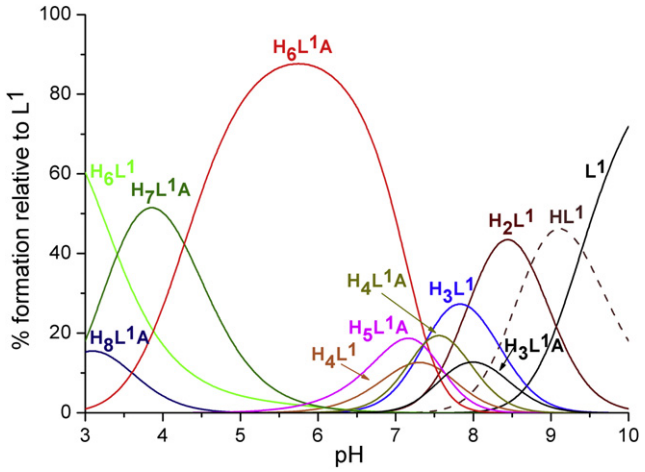

Fig. 2. Species distribution diagram of $(H_nL^1)^{n+}$ in presence of the btc^{3-} anion (A) in H_2O/MeOH (1:1 v/v) solution. The charges were omitted for clarity. $C_{L^1} = C_A = 3 \times 10^{-3}$ mol dm^{-3}.

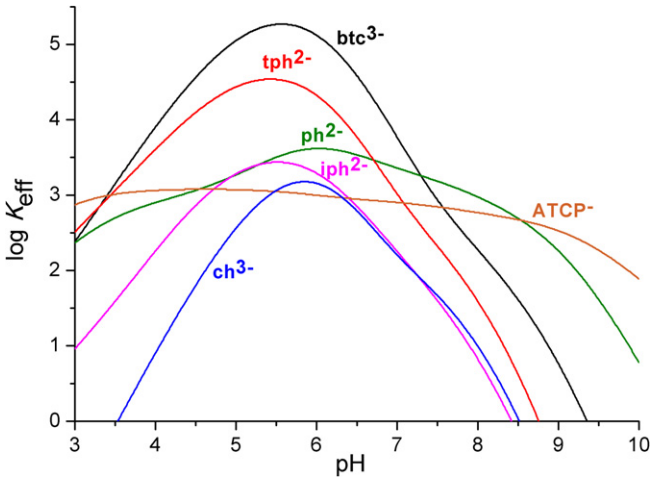

Fig. 3. Plots of log K_{eff} versus pH for the associations between $(H_nL_1)^{n+}$ and the studied anionic substrates in H_2O/MeOH (1:1 v/v) solution. Each curve is identified by the name of the corresponding anion. $C_{L^1} = C_A = 3.0 \times 10^{-3}$ mol dm^{-3}.

indicating that the strengths of the binding do not noticeably change in spite of the deprotonation of the receptor. For the latter two anions, it is possible to consider that the interaction takes only place in one side of the receptor, being expected that the deprotonation of the non-interacting side of the receptor has a small impact on the value of the association constants.

In Table 3 the stepwise association constants are listed based on the results of Tables 1 and 2 and Table S1 of Supplementary data. Equilibria involving the $(H_7L^1)^{7+}$ species only exist at very low pH and the species appear in small percentage, therefore they were not taken into account. For ph^{2-} and ch^{3-} anions, two equilibria were considered for the formation of the $[H_6L^1A]^{(6-i)}$ species, because the values of the corresponding constants are of the same order and probably both are present in solution.

The equilibria involving the completely protonated receptor and the fully deprotonated anion, corresponding to the formation of $[H_6L^1A]^{(6-i)}$ species exhibit the largest values for all the studied anionic substrates. To the associated entity formed on base of such equilibria corresponds stronger interactions, such as electrostatic and hydrogen bonds. The equilibrium between protonated species of the anion and deprotonated forms of the receptor has lower stepwise association constants as expected and observed in Fig. 3. The largest binding constant value was found for the btc^{3-} anionic substrate (log K=5.71, Table 3). In Fig. 3 is observed the maximum log K_{eff} at 5.5 (pH≅5.5), and the apparent discrepancy of values is due to the small amount of $[H_7L^1A]^{4+}$ formed at this pH (see Fig. 2) contributing to the small decrease of the effective constant. Similar situations happen in other cases. Besides btc^{3-}, the receptor has a quite high affinity for tph^{2-} in comparison with the other two structural isomers (iph^{2-} and ph^{2-}), although the differences in affinity are not sufficient for an effective separation for analytical applications. However, the large binding constant for tph^{2-} substrate together with its lowest charge density indicate good structural complementarities in size and binding sites between both partners. Lehn et al.[7,21] reported for the association $[(H_4L^2)tph]^{2+}$ (being L^2 a related compound, see Scheme 1) a binding constant of 4.40 (in log units), which is close to the 4.87 determined in our case (although in different experimental conditions). The X-ray crystal structure of $[(H_4L^2)tph]^{2+}$ showed the tph^{2-} inside the cavity and it was demonstrated that the subunits of the receptor and the anion act cooperatively.[7] Finally, the lowest association constants were found for the less charged (ATCP$^-$) and the aliphatic (ch^{3-}) anions, in spite of the high charge of the latter one. This indicates that both the rigidity and the charge of the substrate are important features in the recognition process and, therefore, modulation of these two factors is required in order to understand the binding recognition.

Unfortunately, our efforts to grow crystals of the associated species adequate for X-ray determinations were not successful, therefore molecular dynamics simulations were performed to go further into the knowledge of the recognition process of these systems, as described below.

2.4. Molecular modelling studies

In spite of the great number of associated entities formed along the pH, the theoretical studies were performed with the completely protonated receptor $(H_6L^1)^{6+}$ and the fully deprotonated anions, A (A=btc^{3-}, tph^{2-} and iph^{2-}), in which the electrostatic interactions are maximized. The conformational analyses of the associated entities formed by $(H_6L^1)^{6+}$ with the anions were performed by quenching molecular dynamics in gas phase (see Experimental section), and they gave the first insights into the receptor flexibility

Table 3
Stepwise association constants ($\log K_{H_hL_lA_a}$) for the equilibria between $(H_nL^1)^{n+}$ and the studied anions (A). I=0.10 mol dm^{-3} in KCl, T=298.2 K

Equilibrium process	ATCP^{-}	ph^{2-}	iph^{2-}	tph^{2-}	btc^{3-}	ch^{3-}
$(H_6L^1)^{6+}+H_2A^{i-} \rightleftarrows [H_8L^1A]^{6-i}$	—	—	—	—	2.89	—
$(H_6L^1)^{6+}+HA^{i-} \rightleftarrows [H_7L^1A]^{(6-i)}$	—	2.69	2.16	3.64	4.57	2.80
$(H_6L^1)^{6+}+A^{i-} \rightleftarrows [H_6L^1A]^{(6-i)}$	3.09	4.05	3.78	4.87	5.71	3.96
$(H_5L^1)^{5+}+HA^{i-} \rightleftarrows [H_6L^1A]^{(5-i)}$	–	3.76	—	—	—	3.77
$(H_5L^1)^{5+}+A^{i-} \rightleftarrows [H_5L^1A]^{(5-i)}$	2.96	3.59	2.91	3.25	4.09	2.44
$(H_4L^1)^{4+}+A^{i-} \rightleftarrows [H_4L^1A]^{(4-i)}$	2.93	2.98	1.92	2.73	3.07	2.16
$(H_3L^1)^{3+}+A^{i-} \rightleftarrows [H_3L^1A]^{(3-i)}$	2.84	2.89	—	—	2.35	—
$(H_2L^1)^{2+}+A^{i-} \rightleftarrows [H_2L^1A]^{(2-i)}$	2.70	—	—	—	—	—
$(HL^1)^{+}+A^{i-} \rightleftarrows [HL^1A]^{(1-i)}$	2.56	—	—	—	—	—

and the molecular recognition processes. In the lowest energy configuration found for $(H_6L^1)^{6+}$, the two tren binding heads are separated by 12.2 Å (the D_{CN}–D_{CN} distance between the centroids defined by the two sets of four nitrogen centres). This value suggests that the macrobicyclic cavity in $(H_6L^1)^{6+}$ is large enough to accommodate the selected carboxylate anions. Indeed in the lowest energy binding arrangements of $[H_6L^1(tph)]^{4+}$ and $[H_6L^1(iph)]^{4+}$, the anion is held inside the receptor cavity through 9 and 10 hydrogen bonding interactions, respectively, with the corresponding N···O=C distances ranging from 2.70–3.22 Å and 2.72–3.29 Å. In addition, the electrostatic interactions between the positive charged receptor and the encapsulated negative anion leads to shorter D_{CN}–D_{CN} distances of 11.42 and 10.96 Å for tph^{2-} and iph^{2-} associations, respectively. In the lowest energy binding scenario of $[H_6L^1(btc)]^{3+}$, the btc^{3-} (Fig. 4) is also inside of the cryptand cavity through nine N–H···O hydrogen bonds established with all six $-NH_2^+$ sites. The corresponding N···O=C distances are between 2.71 and 3.03 Å. However, the D_{CN}–D_{CN} intermolecular distance is diminished to 9.52 Å following the net charge difference between btc^{3-} and iph^{2-} or tph^{2-} anions.

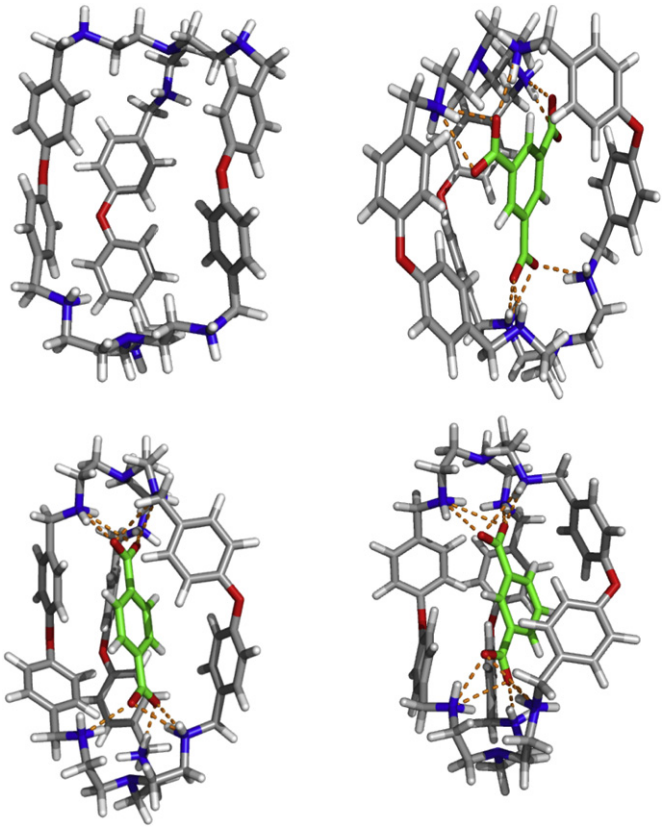

Fig. 4. Lowest energy structures found in the conformational analysis of $(H_6L^1)^{6+}$ (top left) with btc^{3-} (top right), tph^{2-} (down left) and iph^{2-} (down right) with the carbon atoms of the receptor and anion shown in grey and green, respectively. The oxygen, nitrogen and hydrogen atoms are in red, blue and white, respectively. (For interpretation of the references to colour in this figure legend, the reader is referred to the web version of this article).

Subsequently, the dynamic behaviours of the three receptor–anion associations were evaluated submitting the corresponding lowest energy binding arrangements to molecular dynamics (MD) simulations in H_2O/MeOH (1:1 v/v) for 14 ns at 300 K. The MD simulations were performed with the Amber 9 software using the GAFF force field.[26,27]

The variation of the intermolecular distance between the receptor recognition centre, determined with the eight ammonium nitrogen atoms and with three oxygen atoms (C_R), and the mass centre of the anion, determined with the aromatic carbon atoms (C_A), along the simulation time are plotted in Fig. 5 for the three anion associations. Different dynamic structural behaviours were observed. The btc^{3-} anion is slightly inserted into the cryptand cavity over the entire time of simulation leading to $C_R\cdots C_A$ average distance of 4.42 Å. In contrast, the tph^{2-} anion stays encapsulated going to the border during few periods of picoseconds, but never leaving the cryptand cavity. The average $C_R\cdots C_A$ distance is 1.11 Å. The iph^{2-} anion has an intermediate binding behaviour with the anion leaving the receptor cavity for 1.5 ns, between 2.5 and 4.0 ns of MD simulation, but during this short period it is still hydrogen bonded at least to one $-NH_2^+$ binding group. The $C_R\cdots C_A$ average distance is 1.98 Å. The molecular recognition processes between $(H_6L^1)^{6+}$ and the three anions are illustrated in Fig. 6 with snapshots taken from the corresponding MD simulations. In addition, the simulations of the three anion associations were repeated three times using different starting structures and different initial seed velocities. The results obtained were equivalent to those reported here, which validates our MD simulations.

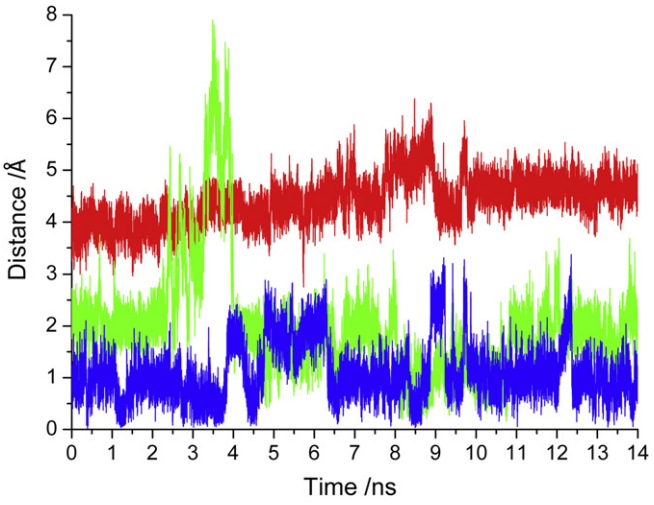

Fig. 5. Evolution of the $C_R\cdots C_A$ distance for btc^{3-} (red), tph^{2-}(blue) and iph^{2-} (green) substrates during the MD simulations. (For interpretation of the references to colour in this figure legend, the reader is referred to the web version of this article).

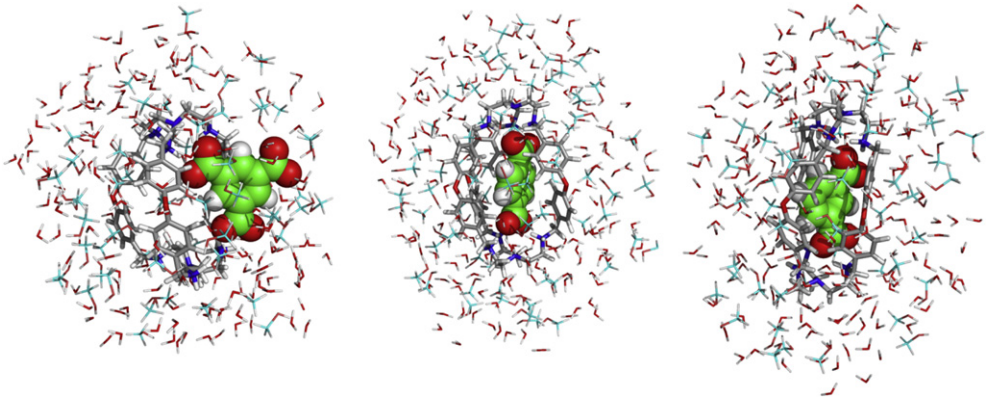

Fig. 6. Snapshots of $(H_6L^1A)^{i+}$ assembled entities taken at 10.5 ns of MD simulation for btc^{3-} anion (left), tph^{2-} (centre) and iph^{2-} (right). Only the closest solvent molecules within 8 Å distance from $(H_6L^1)^{6+}$ are shown. Atom colour scheme used as given in Fig. 4 apart of the carbon atoms of MeOH molecules, which are drawn in light blue. (For interpretation of the references to colour in this figure legend, the reader is referred to the web version of this article).

The interactions established either by the receptor or the anions with methanol and water solvent molecules play an important role in the association process, as can be seen from the radial distribution functions (rdfs) for O–H···C_R and O–H···O_A distances between the solvent molecules and the receptor recognition centre (C_R) and the carboxylate binding centres (O_A), respectively. The C_R definition is given above while O_A is the mass centre determined by two oxygen atoms of each carboxylate group. In Fig. S3 given in Supplementary data are plotted the rdfs calculated for O–H···O_A distances between methanol or water solvent molecules and the three associated anions. The three anions are solvated preferentially by water molecules rather than by the methanol molecules, but this solvation preference is much lesser pronounced for tph^{2-}, which is taking into account that the anion remains almost encapsulated for 14 ns of MD simulation, becoming the anion lesser accessible to both types of solvent molecules. From these rdfs is also apparent that the carboxylate binding centres are not equally solvated. In particular for btc^{3-}, the solvent molecules surround preferentially the carboxylate group lesser involved in hydrogen bonding interactions with the receptor, although this effect is lesser pronounced for the methanol solvent molecules. Furthermore, considering the methanol and water solvent molecules together, the btc^{3-} is the more solvated anion followed by iph^{2-} and tph^{2-} in agreement with the anions position relative to the receptor. The rdfs calculated with water molecules exhibit two well-defined water shells centred at ca. 1.75 and 2.95 Å, respectively. The first one is the more intense and is straight associated with the formation of O–H···O=C hydrogen bonds between the anions and water molecules. The rdfs of methanol exhibit four solvent coordination shells with the first one occurring at ca. 1.65 Å. This solvation shell is the strongest one and it is due to O–H···O=C hydrogen bonding interactions. A further analysis of the intermolecular distances between the individual nitrogen binding sites of the receptor and oxygen atoms of the carboxylate groups recorded during the course of MD simulations is presented in Supplementary data.

The rdfs for O–H···C_R distances between methanol or water solvent molecules and $(H_6L^1)^{6+}$, presented in Fig. S4 of Supplementary data, show two solvent shells, the first one occurs at ca. 2.85 Å for btc^{3-}, 2.95 Å for iph^{2-} and 2.75 Å for tph^{2-}. The first methanol coordination shell is centred at ca. 2.95 Å for btc^{3-} and tph^{2-}, and at 2.85 Å for iph^{2-}. As observed for anions, the protonated receptor is also solvated in lesser extension by methanol, see Supplementary data.

Generally, the absolute binding free energy of the substrate can be estimated from MD collected structures through the MM/PBSA (Molecular Mechanics Poisson–Boltzmann surface area) approach[28] using the following equation:

$$\Delta G_{bind} = G_{interaction} - G_{receptor} - G_{substrate} = \Delta E_{MM} + \Delta G_{PB} + \Delta G_{SA} - T\Delta S$$

where ΔE_{MM} is the molecular mechanics interaction energy between the receptor and substrate; ΔG_{PB} and ΔG_{SA} represent the polar and non-polar components of the solvation free energy, respectively; $T\Delta S$ is the solute entropy contribution at temperature T. All these terms can be computed with the Amber using the appropriate methods. The largest contributors to the binding free energy (ΔG_{bind}) of associations between high charged species are the ΔE_{MM} and ΔG_{PB} terms. The ΔG_{PB} contribution is calculated with numerical solution of Poisson–Boltzmann equation considering continuum solvent model, typically water. However, this method is not applicable to estimate the electrostatic contribution to the free energy in complex solvent systems, such as the solvent mixture H_2O/MeOH (1:1 v/v) used in the current work. Therefore our calculations using the MM-PBSA script implement in Amber were limited to computing the ΔE_{MM} term, which is mainly composed of electrostatic and van der Waals energy components ($\Delta E_{MM} \approx \Delta E_{ele} + \Delta E_{vdw}$), when the receptor and anion keep almost their free structures upon binding.

In Fig. S5 of Supplementary data are plotted the evolution of ΔE_{MM} interaction energy for the btc^{3-}, tph^{2-} and iph^{2-} anion associations for the 14 ns long MD simulation as well as the corresponding individual electrostatic terms. These molecular mechanic energies were calculated using just the snapshots taken from MD trajectory on the anion–receptor association. As expected, the negative ΔE_{ele} component is the largest contributor for the stabilization of anion associations to $(H_6L^1)^{6+}$, being the attractive contribution of ΔE_{vdw} negligible. In addition, the average ΔE_{ele} energies of the anion associations are in kcal mol^{-1}: −880.9 for btc^{3-}, −621.5 for iph^{2-} and −706.5 for tph^{2-}. These values are entirely consistent with the experimental binding affinity order $btc^{3-} > iph^{2-} > tph^{2-}$ indicating that it is mainly dictated by the magnitude of electrostatic interactions, which incorporate the hydrogen bonding interactions in the GAFF force field. In all three binding associations, the negative ΔE_{ele} term is partially counterbalanced by a positive ΔG_{PB} term, which is necessarily bigger for the btc^{3-} association given that the corresponding ΔE_{ele} term is the largest one.

Subsequently, the binding affinity of $(H_6L^1)^{6+}$ towards btc^{3-} and iph^{2-} anions was estimated by free energy calculations via thermodynamic integration method[29] from two independent long simulations carried out in H_2O/MeOH. In the first one the free btc^{3-} anion was mutated into iph^{2-} and in the second one the $[H_6L^1(btc)]^{3+}$ association was mutated into $[H_6L^1(iph)]^{4+}$. Both transformations were performed using a single topology

perturbation approach as described in Experimental section. The relative binding free energy associated with the first and second transformation are 50.51 and 52.81 kcal mol^{-1}, respectively, leading to a relative binding free energy ($\Delta\Delta G=\Delta G_{interaction}-\Delta G_{anion}$) of 2.3±0.8 kcal mol^{-1}, which is close to the determined from the experimental potentiometric data ($\Delta\Delta G$=2.62 kcal/mol).

3. Conclusions

The binding ability of the receptor $(H_nL^1)^{n+}$ for several carboxylate anions was evaluated using potentiometric measurements in H_2O/MeOH (1:1 v/v) solution. The effective constants at pH 5.5 follow the order $btc^{3-}>tph^{2-}>ph^{2-}\approx iph^{2-}>ch^{3-}\approx ATCP^{-}$. Further, the molecular recognition processes of btc^{3-}, tph^{2-} and iph^{2-} anions with $(H_6L^1)^{6+}$ were studied via molecular dynamics simulations. These studies revealed that the tph^{2-} remained encapsulated over the entire time of simulation while the btc^{3-} is partially inserted into the receptor cavity with one carboxylate group largely exposed to water solvent molecules, and iph^{2-} anion exhibited an intermediate binding behaviour. In fact, the tricarboxylate anion is solvated in more extension by water and methanol molecules than the dicarboxylate anions revealing the importance of the solvent in the recognition process. The free energy difference between btc^{3-} and iph^{2-} associations estimated by free energy calculations is in excellent agreement with the difference found from the experimental values for the corresponding association constants, which indicates that the unconstrained molecular dynamics simulations carried out with these two anions are realistic pictures of their molecular recognition processes. The binding affinity of btc^{3-}, iph^{2-} and tph^{2-} to $(H_6L^1)^{6+}$ is dictated by a delicate balance between the electrostatic interactions and the solvation of the anion association. This is particularly evident for the $[H_6L^1(btc)]^{3+}$ association, in which the btc^{3-} located above the cryptand cavity is more exposed to the solvent molecules, but presents the larger association constant due to electrostatic attraction between the receptor and anion, which have net charges of +6 and −3, respectively.

4. Experimental section

4.1. General

Microanalyses were carried out by the ITQB Microanalytical Service. The ^{1}H and ^{13}C NMR spectra were recorded in a Bruker CXP 300 spectrometer.

4.2. Reagents

p-Tolylether, diethelenetriamine (dien) and tris(2-aminoethyl) amine (tren) were obtained from Aldrich, *N*-bromosuccinimide and hexamethylenetetramine from Merck, 2,2′-azobis(2-methyl-propionitrile) from Acros Organics and benzoyl peroxide from Fluka. 1,3,5 Benzenetricarboxylic acid, terephthalic acid (98%), phthalic acid (>99.5%), isophthalic acid (99%), 1,3,5-cyclohexanetricarboxylic acid (95%) and aminotricloropyridine (98%) were purchased from Aldrich. The 4-(4-formylphenoxy)benzaldehyde was synthesized using the procedure described.[22] All chemicals were of reagent grade and used as supplied. The reference used for the ^{1}H NMR spectra in D_2O was 3-(trimethylsilyl)propanoic acid-d_4 sodium salt. For ^{13}C NMR spectra dioxane was used as internal reference.

4.3. Synthesis of L^1

To a solution of tris(2-aminoethyl)amine (1.33 mmol, 0.2 cm^3) in acetonitrile (30 cm^3) was added during a period of 1 h a solution of of 4-(4-formylphenoxy)benzaldehyde (2.0 mmol, 0.452 g) also in acetonitrile (24 cm^3). The mixture was left to stir at rt under N_2 overnight. The white precipitate then formed was separated, dried and dissolved in ethanol (10 cm^3). Then $NaBH_4$ 0.25 g (6.7 mmol) was added in four portions and the mixture was left to reflux for 6 h. The insoluble white solid was separated. The solution was evaporated, dissolved in water and extracted with CH_2Cl_2 (6×20 cm^3). Evaporation of the organic phase gave rise to oil, which was dissolved in ethanol. ^{1}H NMR ($CDCl_3$, ppm): δ 6.88 (8H, d), 6.59 (8H, d), 3.55 (8H, s), 2.68 (12H, t), 2.59 (12H, t). ^{13}C NMR ($CDCl_3$, ppm) δ 155.7, 134.8, 128.9, 118.3, 54.4, 53.3, 47.9. ESI-MS *m*/*z*: $[M+2H]^{2+}$=438.40, $[M+3H]^{3+}$=292.5.

The addition of HBr solution (49%) to the latter solution led to a white precipitate of the desired macrobicycle in its hexaprotonated form. Yield of $[H_6L^1]^{6+}$: 33 mmol (30%). Mp 200–203 °C. ^{1}H NMR (D_2O, ppm): δ 7.49 (d, *J*(H,H)=8.6 Hz, 8H), 7.13 (d, *J*(H,H)=8.6 Hz, 8H), 4.22 (8H, s), 3.16 (t, *J*(H,H)=6.2 Hz, 12H), 2.84 (t, *J*(H,H)=6.2 Hz, 12H). ^{13}C NMR (D_2O, ppm) δ 159.8, 134.6, 128.9, 121.9, 52.9, 52.3, 46.6. ESI-MS *m*/*z*: $[M+2H]^{2+}$=438.40, $[M+3H]^{3+}$=292.5. Calcd for $C_{54}H_{72}Br_6N_8O_3\cdot 4H_2O$: C, 45.27; H, 5.63; N, 7.82. Found: C, 45.13; H, 5.77; N, 7.76.

4.4. Potentiometric measurements

4.4.1. Reagents and solutions. Aromatic anions were prepared from the respective acids by addition of 2 or 3 equiv of KOH in aqueous solution. The solutions were evaporated and the solid recrystallized from acetone. The anions were then standardized by titration using a standard HCl solution. The cyclohexanetricarboxylic acid and the 4-amino-3,5,6-trichloro-2-pyridine carboxylic acid were used in the acid form, and standardized by titration with standard KOH. The carbonate-free solutions of KOH were freshly prepared, maintained in a closed bottle and discarded when the percentage of carbonate was about 0.5% of the total amount of base (verified with the Gran method).[30,31] All the solutions were prepared in H_2O/MeOH (1:1, v/v). The methanol was purified by standard methods[32] and the demineralized water used was obtained from a Millipore/Milli-Q system.

4.4.2. Equipment and working conditions. The equipment used was described before.[20] The glass electrode was pre-treated by soaking it in H_2O/MeOH (1:1 v/v) solution for one week in order to prevent erratic responses. The temperature was kept at 298.2±0.1 K; atmospheric CO_2 was excluded from the cell during the titration by passing purified argon across the top of the solution in the reaction cell. The ionic strength of the solutions was kept at 0.10 mol dm^{-3} in KCl.

The $[H^+]$ of the solutions was determined by the measurement of the electromotive force of the cell, $E=E^{o\prime}+Q\log[H^+]+E_j$. $E^{o\prime}$, Q, E_j and $K_w=([H^+][OH^-])$ were obtained as described previously.[33] The term pH is defined as $-\log[H^+]$. The value of K_w was found to be equal to $10^{-13.91}$ under our experimental conditions, in agreement with that determined by Rochester.[34]

The potentiometric equilibrium measurements were carried out using 20.00 mL of $\approx 2.00\times10^{-3}$ mol dm^{-3} solutions diluted to a final volume of 32.00 cm^3, in the absence of anions, in the presence of anion ions in 1:1, 2:1 and 4:1 C_A/C_R ratios. A minimum of two replicates was undertaken. All the anions were independently titrated in the same experimental conditions. A correction was made for the small decrease in volume, which occurs on mixing methanol and water. Care has been taken to maintain unaltered the methanol/water ratio in measured solution.

4.4.3. Calculation of equilibrium constants. Overall protonation constants, β_i^H, for the receptor and all the anions were calculated by fitting the potentiometric data obtained for all the performed titrations with the HYPERQUAD program.[23] All these constants were taken as fixed values to obtain the equilibrium constants of the new

species from the experimental data corresponding to all the titrations at different $C_{L^1} : C_A$ ratios, using also the HYPERQUAD program. The initial computations were obtained in the form of overall stability constants, $\beta_{H_hL_lA_a}$ values, $\beta_{H_hL_lA_a} = [H_hL_lA_a]/[H]^h[L]^l[A]^a$. The errors quoted are the standard deviations of the overall association constants given directly by the program for the input data, which include all the experimental points of all titration curves. The species considered in a particular model were those that could be justified by the principles of supramolecular chemistry.

The associated constants of $(H_nL^1)^{n+}$ with the different anions were determined from a minimum of 100 (for tph^{2-}) to 223 (for iph^{2-}) experimental points, and a minimum of two titration curves.

4.5. Molecular modelling

All MD simulations and subsequent free energy calculations were carried out with the Amber 9 suite of programs,[26] using parameters for the aromatic anions (btc^{3-}, tph^{2-} and iph^{2-}) and receptor taken from the Gaff force field.[27] The methanol solvent molecules were described using a full atom solvent model with atomic charges and force field parameters taken from Ref. 35. A TIP3P model was used for the water.[36] The chloride ion with a charge of −1 was described with van der Waals parameters taken from Ref. 37.

The starting geometry of $(H_6L^1)^{6+}$ was generated from unpublished crystal structure of $C_{54}H_{80}N_8O_7Br_6$ salt.[38] Partial atomic charges for the receptor and for the anions were calculated at the HF/6-31G* level by means of RESP methodology using the Gaussian 03 program.[39] The docking between the receptor and each anion was performed through the quenched molecular dynamics as follows. The anion was positioned inside the cryptand cavity and subsequently the association model was minimized by molecular mechanics (MM). The minimized structure was then subjected in gas phase to a molecular dynamic (MD) quenching run at 2000 K using a time step of 1 fs. 50,000 conformations were generated at 0.1 ps intervals and they were minimized by MM via conjugate gradients until the convergence was achieved using an appropriated house script. The energetic convergence criterion was 0.0001 kcal mol^{-1}. The lowest energy geometric arrangements found for the association entities of $(H_6L^1)^{6+}$ with btc^{3-}, tph^{2-} and iph^{2-} anions were solvated with previous H_2O/MeOH (1:1 v/v) equilibrated box. Three or four chloride anions were placed outside of the receptor to balance the charge. The solvated systems were equilibrated under periodic boundary conditions using the following multistage protocol. The equilibration process started with the minimization of water molecules and chloride counter-ions by MM with 10,000 steps by the steepest descent method followed by 10,000 steps of conjugate gradients keeping the structure of the supramolecular association rigid with positional restrain of 500 kcal mol^{-1} $Å^{-2}$. Then, the restrain was removed and the entire system was allowed to relax. After minimization process, the solvated system was heated up to 300 K over 50 ps in an NVT ensemble with a weak positional restrain on the binding complex of 10 kcal mol^{-1} $Å^{-2}$. Subsequently the positional restrain was removed and the equilibration followed with a MD simulation run of 500 ps at 300 K and an average pressure of 1 atm in order to adjust the density of the cubic box to the expected value for the solvent mixture. At this stage the average value for density remained constant, at least during the last 100 ps. Finally, for each supramolecular association, a data collection run was carried out for 14 ns using an NPT ensemble. Snapshots were saved every 0.2 ps. Bond lengths involving all bonds to hydrogen atoms were constrained with the SHAKE algorithm[40] allowing the use of a time step of 2 fs. The Particle Mesh Ewald method[41] was used to treat the long-range electrostatic interactions and the non-bonded van der Waals interactions were truncated with a 12 Å cut-off.

The relative free binding energy ($\Delta\Delta G = \Delta G_{interaction} - \Delta G_{anion}$) of the receptor to btc^{3-} and iph^{2-} anions in H_2O/MeOH (1:1 v/v) was calculated from the relative free energies associated with $btc^{3-} \rightarrow iph^{2-}$ mutation in solution (ΔG_{anion}) and in anion association ($\Delta G_{interaction}$), respectively. These two energies were obtained by means of thermodynamics integration[29] as follows. The mutation simulations were divided into 21 windows (λ=0, 0.05, 0.10…1) each consisting of 100 ps MD equilibration and a 250 ps data collection, carried out at 300 K and 1 atm using the previously equilibrated system. The $btc^{3-} \rightarrow iph^{2-}$ transformation in association and in solution was carried out annihilating one carboxylate group carried out in two steps. In the first one, the atomic charges were changed with the total charge going from −3 to −2. In the second step, the van der Walls parameters were transformed.

Supplementary data

Protonation constants ($\log \beta_{H_hA_a}$) of all the studied anions; variations in $N_i \cdots O_j$ distances (Å) of $[H_6L^1A]^{n+}$ MD simulations (A=btc^{3-}, tph^{2-} and iph^{2-}); ^1H NMR and ^{13}C NMR spectra of the cryptand L^1 in $CDCl_3$; ^1H NMR spectrum of the cryptand L^1 in D_2O; rdfs for $O-H \cdots O_A$ distances between the water and methanol molecules and the mass centre determined by two oxygen atoms of each carboxylate groups for btc^{3-}, tph^{2-} and iph^{2-} associations; rdfs for $O-H \cdots C_R$ distances between the water and methanol molecules and the receptor recognition centre in the associations; evolution of the molecular mechanics interaction energies for the btc^{3-}, tph^{2-} and iph^{2-} associations with $(H_6L^1)^{6+}$ during the course of the MD simulations; atomic coordinates (mol format) of the binding scenarios shown in Figs. 4 and 6. Supplementary data associated with this article can be found in the online version, at doi:10.1016/j.tet.2010.09.006. These data include MOL files and InChiKeys of the most important compounds described in this article.

References and notes

1. Bianchi, A.; Bowman-James, K.; Garcia-España, E. *Supramolecular Chemistry of Anions*; John Wiley & Sons: New York, NY, 1997; Steed, J. W.; Atwood, J. L. *Supramolecular Chemistry*, 2nd ed.; John Wiley & Sons: Chichester, UK, 2009.
2. Schneider, H.-J.; Yatsimirsky, A. K. *Chem. Soc. Rev.* **2008**, *37*, 263–277.
3. García-España, E.; Díaz, P.; Llinares, J. M.; Bianchi, A. *Coord. Chem. Rev.* **2006**, *250*, 2952–2986.
4. Mateus, P.; Bernier, N.; Delgado, R. *Coord. Chem. Rev.* **2010**, *254*, 1726–1747.
5. Mateus, P.; Delgado, R.; Brandão, P.; Félix, V. *J. Org. Chem.* **2009**, *74*, 8638–8646.
6. Mateus, P.; Delgado, R.; Brandão, P.; Carvalho, S.; Félix, V. *Org. Biomol. Chem.* **2009**, *7*, 4661–4673.
7. Lehn, J.-M.; Méric, R.; Vigneron, J. P.; Bkouche-Waksman, I.; Pascard, C. *Chem. Commun.* **1991**, 62–64.
8. Saeed, M. A.; Fronczek, F. R.; Huanga, M.-J.; Hossain, M. A. *Chem. Commun.* **2010**, *46*, 404–406.
9. Hynes, M. J.; Maubert, B.; McKee, V.; Town, R. M.; Nelson, J. *J. Chem. Soc., Dalton Trans.* **2000**, 2853–2859.
10. Ravikumar, I.; Lakshminarayanan, P. S.; Suresh, E.; Ghosh, P. *Inorg. Chem.* **2008**, *47*, 7992–7999.
11. Bazzicalupi, C.; Bencini, A.; Bianchi, A.; Danesi, A.; Giorgi, C.; Lorente, M. A. M.; Valtancoli, B. *New J. Chem.* **2006**, *30*, 959–965.
12. Arunachalam, M.; Ravikumar, I.; Ghosh, P. *J. Org. Chem.* **2008**, *73*, 9144–9147.
13. Kang, S. O.; Day, V. W.; Bowman-James, K. *J. Org. Chem.* **2010**, *75*, 277–283.
14. Kang, S. O.; Day, V. W.; Bowman-James, K. *Org. Lett.* **2008**, *10*, 2677–2680.
15. Nelson, J.; Nieuwenhuyzen, M.; Pál, I.; Town, R. M. *Dalton Trans.* **2004**, 2303–2308.
16. Korendovych, I. V.; Cho, M.; Makhlynets, O. V.; Butler, P. L.; Staples, R. J.; Rybak-Akimova, E. V. *J. Org. Chem.* **2008**, *73*, 4771–4782.
17. Fitzmaurice, R. J.; Kyne, G. M.; Douheret, D.; Kilburn, J. D. *J. Chem. Soc., Perkin Trans. 1* **2002**, 841–864.
18. Bencini, A.; Bianchi, A.; Burguete, M. I.; Dapporto, P.; Doménech, A.; García-España, E.; Luis, S. V.; Paoli, P.; Ramírez, J. A. *J. Chem. Soc., Perkin Trans. 2* **1994**, 569–577.
19. Carvalho, S.; Delgado, R.; Fonseca, N.; Félix, V. *New J. Chem.* **2006**, *30*, 247–257.
20. Carvalho, S.; Delgado, R.; Drew, M. G. B.; Calisto, V.; Félix, V. *Tetrahedron* **2008**, *64*, 5392–5403.
21. Jazwinski, J.; Lehn, J.-M.; Lilienbaum, D.; Ziessel, R.; Guilhem, J.; Pascard, C. *J. Chem. Soc., Chem. Commun.* **1987**, 1691–1694.

22. Gonilho, L. M. A. F. C. PhD thesis, Instituto Superior Técnico, Lisboa, Portugal, 2000.
23. Gans, P.; Sabatini, A.; Vacca, A. *Talanta* **1996**, *43*, 1739–1753.
24. Hodacová, J.; Chadim, M.; Závada, J.; Aguilar, J.; Garcia-España, E.; Luis, S. V.; Miravet, J. F. *J. Org. Chem.* **2005**, *70*, 2042–2047.
25. Albelda, M. T.; Bernardo, M. A.; Garcia-España, E.; Godino-Salido, M. L.; Santiago, V. L.; Melo, M. J.; Pina, F.; Soriano, C. *J. Chem. Soc., Perkin Trans. 2* **1999**, 2545–2549.
26. Case, D. A.; Darden, T. A.; Cheatham, T. E. I.; Simmerling, C. L.; Wang, J.; Duke, R. E.; Luo, R.; Merz, K. M.; Pearlman, D. A.; Crowley, M.; Walker, R. C.; Zhang, W.; Wang, B.; Hayik, S.; Roitberg, A.; Seabra, G.; Wong, K. F.; Paesani, F.; Wu, X.; Brozell, S.; Tsui, V.; Gohlke, H.; Yang, L.; Tan, C.; Mongan, J.; Hornak, V.; Cui, G.; Beroza, P.; Mathews, D. H.; Schafmeister, C.; Ross, W. S.; Kollman, P. A. *Amber 9*; University of California: San Francis, CA, 2006.
27. Wang, J.; Wolf, R. M.; Caldwell, J. W.; Kollmann, P. A.; Case, D. A. *J. Comput. Chem.* **2004**, *25*, 1157–1174.
28. Kollman, P. A.; Massoca, I.; Kuhn, B.; Huo, S.; Chong, L.; Lee, M.; Lee, T.; Duan, Y.; Wang, W.; Donni, O.; Cieplak, P.; Srinivasan, J.; Case, D. A.; Cheathamm, T. E., III. *Acc. Chem. Res.* **2000**, *33*, 889–897.
29. Chipot, C.; Pohorille, A. *Free Energy Calculations, Theory and Applications in Chemistry and Biology*; Springer: Berlin, 2007.
30. Gran, G. *Analyst (London)* **1952**, *77*, 661–671.
31. Rossotti, F. J.; Rossotti, H. J. *J. Chem. Educ.* **1965**, *42*, 375–378.
32. Perrin, D. D.; Armarego, W. L. F. *Purification of Laboratory Chemicals*, 3rd ed;; Pergamon: Oxford, 1988.
33. Li, F.; Delgado, R.; Drew, M. G. B.; Félix, V. *Dalton Trans.* **2006**, 5396–5403.
34. Rochester, C. H. *J. Chem. Soc., Dalton Trans.* **1972**, 5–8.
35. Caldwell, J. W.; Kollman, P. A. *J. Phys. Chem.* **1995**, *99*, 6208–6219.
36. Jorgensen, W. L.; Chandrasekhar, J.; Madura, J. D.; Impey, R. W.; Klein, M. L. *J. Chem. Phys.* **1983**, *79*, 926–935.
37. Blas, J. R.; Marquez, M.; Sessler, J. L.; Luque, F. J.; Orozco, M. *J. Am. Chem. Soc.* **2002**, *124*, 12796–12805.
38. Crystal data of $[(H_6L^1)Br]5Br\cdot 4H_2O$. Triclinic, space group $P\bar{1}$, Z=2, a=13.1026(2), b=15.1074(19), c=18.6241(28) A, α=72.282(12), β=82.183(2), γ=8.394(12)°, V=3468.5(9) Å^3. The single crystal X-ray data were collected on a CCD Bruker APEX II at 150(2) K using graphite monochromatized Mo Kα radiation (λ=0.71073 Å); 19,538 reflections were collected and subsequently used in solution and the structure refinement. The crystal structure was solved until R value of 0.098 was achieved. The structure was unequivocally determined showing a bromide anion inserted into the $(H_6L^1)^{6+}$ binding pocket. However, the bromide counter-ions as well as the solvent water molecules with fractional occupation factors were found disordered over several positions. Different trial refinement models were experimented, but unfortunately, it was not possible to find one with acceptable chemical sense. By this reason the single crystal structure determination is not reported here.
39. Frisch, M. J.; Trucks, G. W.; Schlegel, H. B.; Scuseria, G. E.; Robb, M. A.; Cheeseman, J. R.; Montgomery, J. A., Jr.; Vreven, T.; Kudin, K. N.; Burant, J. C.; Millam, J. M.; Iyengar, S. S.; Tomasi, J.; Barone, V.; Mennucci, B.; Cossi, M.; Scalmani, G.; Rega, N.; Petersson, G. A.; Nakatsuji, H.; Hada, M.; Ehara, M.; Toyota, K.; Fukuda, R.; Hasegawa, J.; Ishida, M.; Nakajima, T.; Honda, Y.; Kitao, O.; Nakai, H.; Klene, M.; Li, X.; Knox, J. E.; Hratchian, H. P.; Cross, J. B.; Bakken, V.; Adamo, C.; Jaramillo, J.; Gomperts, R.; Stratmann, R. E.; Yazyev, O.; Austin, A. J.; Cammi, R.; Pomelli, C.; Ochterski, J. W.; Ayala, P. Y.; Morokuma, K.; Voth, G. A.; Salvador, P.; Dannenberg, J. J.; Zakrzewski, V. G.; Dapprich, S.; Daniels, A. D.; Strain, M. C.; Farkas, O.; Malick, D. K.; Rabuck, A. D.; Raghavachari, K.; Foresman, J. B.; Ortiz, J. V.; Cui, Q.; Baboul, A. G.; Clifford, S.; Cioslowski, J.; Stefanov, B. B.; Liu, G.; Liashenko, A.; Piskorz, P.; Komaromi, I.; Martin, R. L.; Fox, D. J.; Keith, T.; Al-Laham, M. A.; Peng, C. Y.; Nanayakkara, A.; Challacombe, M.; Gill, P. M. W.; Johnson, B.; Chen, W.; Wong, M. W.; Gonzalez, C.; Pople, J. A. *Gaussian 03, Revision C.02*; Gaussian: Wallingford, CT, 2004.
40. Ryckaert, J. P.; Cicotti, G.; Berendsen, H. J. C. *J. Comput. Phys.* **1977**, *23*, 327–342.
41. Essmann, U.; Perera, L.; Berkowitz, M. L.; Darden, T.; Lee, H.; Pedersen, L. G. *J. Chem. Phys.* **1995**, *103*, 8577–8593.